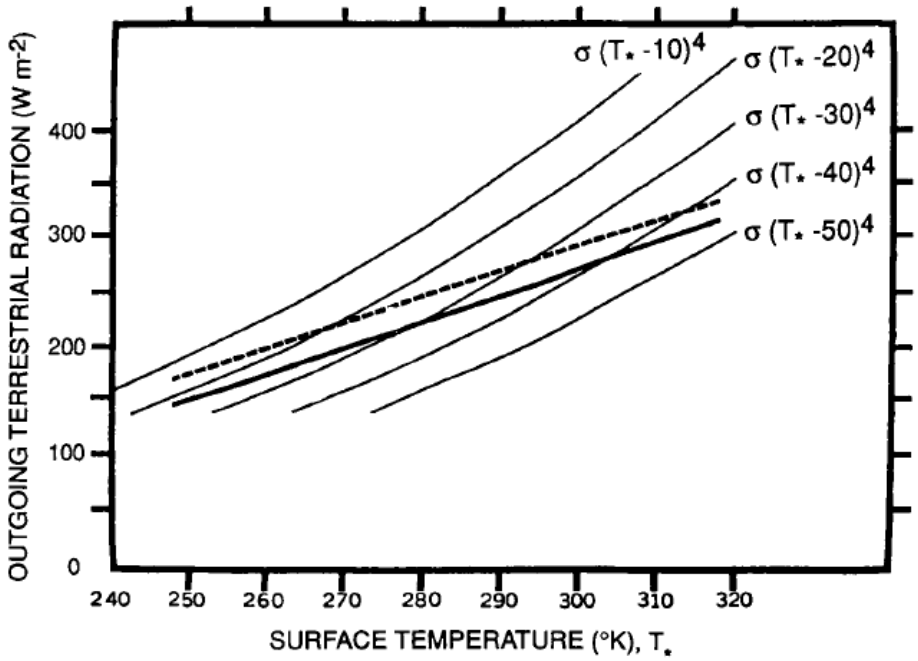

Fig. 9.1 Graph of outgoing terrestrial emission at the top of the atmosphere as a function of surface temperature calculated from a radiative–convective equilibrium model in which the relative humidity is kept fixed so that the specific humidity increases with temperature. For comparison, Stefan–Boltzmann emission curves are shown for temperatures equal to the surface temperature T_*, minus fixed amounts from 10 to 50°C. The dashed line is for clear skies and the solid line is for average cloudiness. [Adapted from Manabe and Wetherald (1967). Reprinted with permission from the American Meteorological Society.]

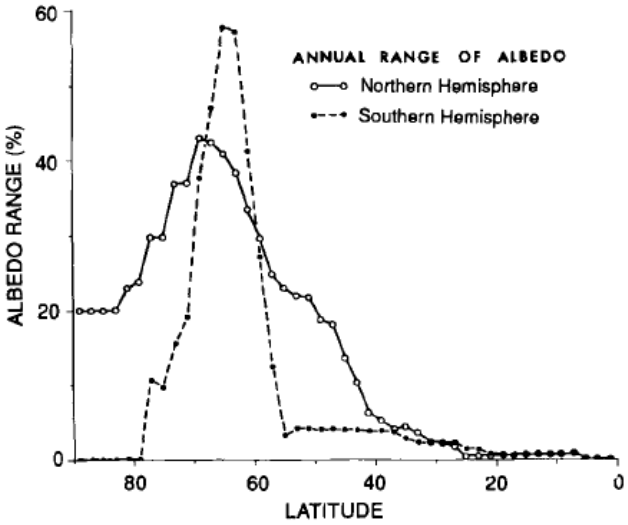

Fig. 9.2 Graph of the annual range of surface albedo in the Northern and Southern Hemispheres. The largest annual ranges occur in the latitude range of Antarctic sea ice in the Southern Hemisphere and sea ice and snowcover in the Northern Hemisphere. [From Kukla and Robinson (1980). Reprinted with permission from the American Meteorological Society.]

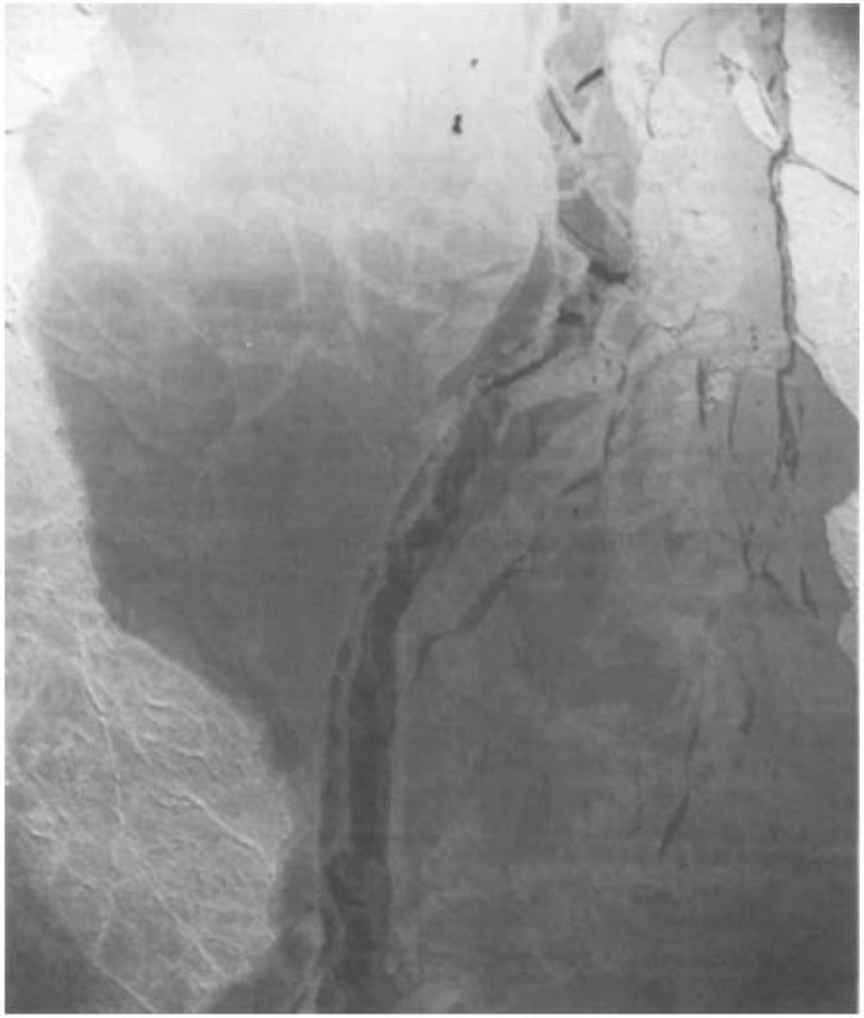

Fig. 9.3 Aerial photograph of sea ice in the Arctic, showing the relationship of albedo to ice thickness and snowcover. A large lead has refrozen with a thin layer of ice that has reopened and fingered. Fingering occurs when thin layers of ice are pushed together and slide over the top of each other. The darkest areas are open water. Image is about 15 km across. [Photo: U.S. Navy (NAVOCEANO), 1972.]

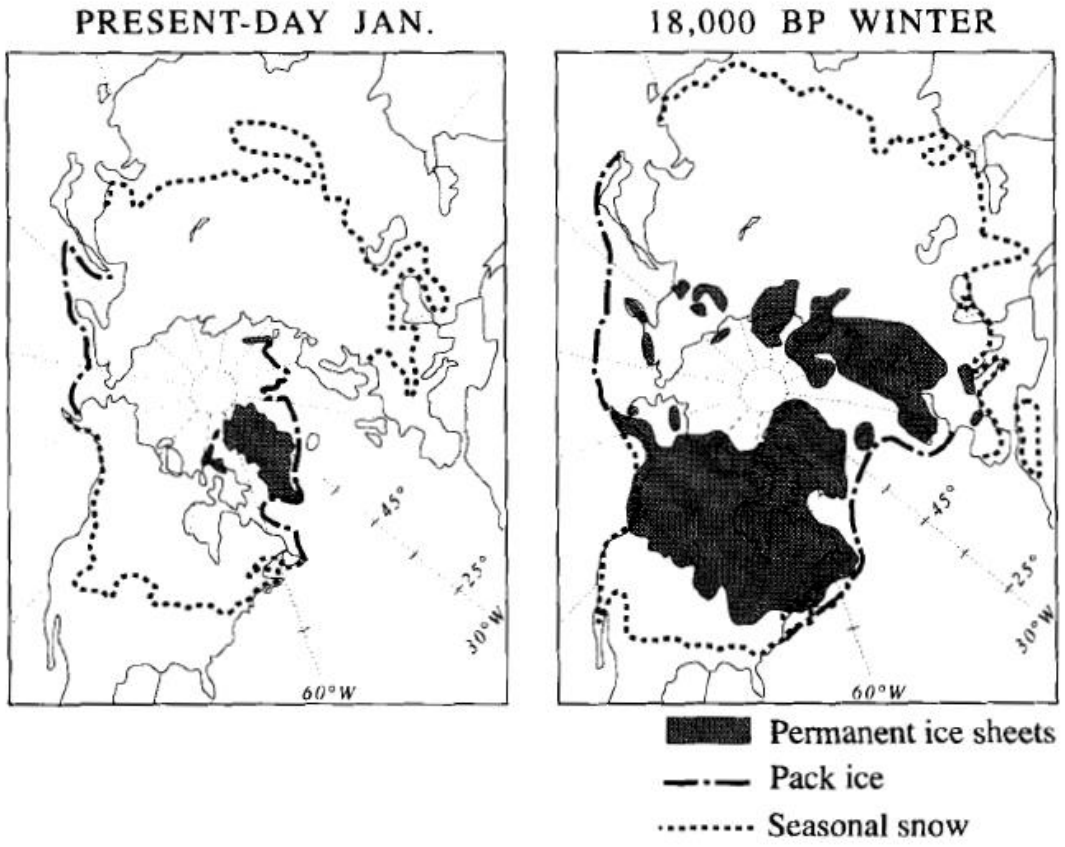

Fig. 9.4 Extent of permanent ice sheets (shaded), seasonal snowcover (dotted line), and pack ice (perennial sea ice, dash–dot line) at present and estimated for the last glacial maximum. [From Robinson, unpublished, as published in Kukla (1979).]

Ice-Albedo feedback

A positive feedback

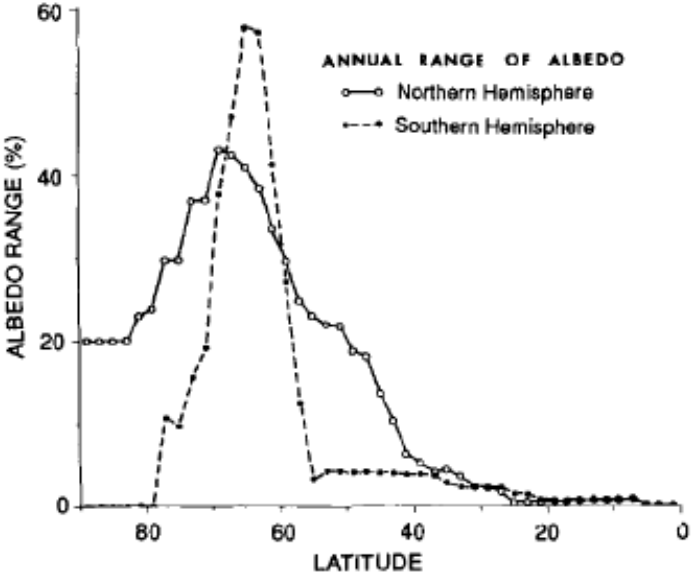

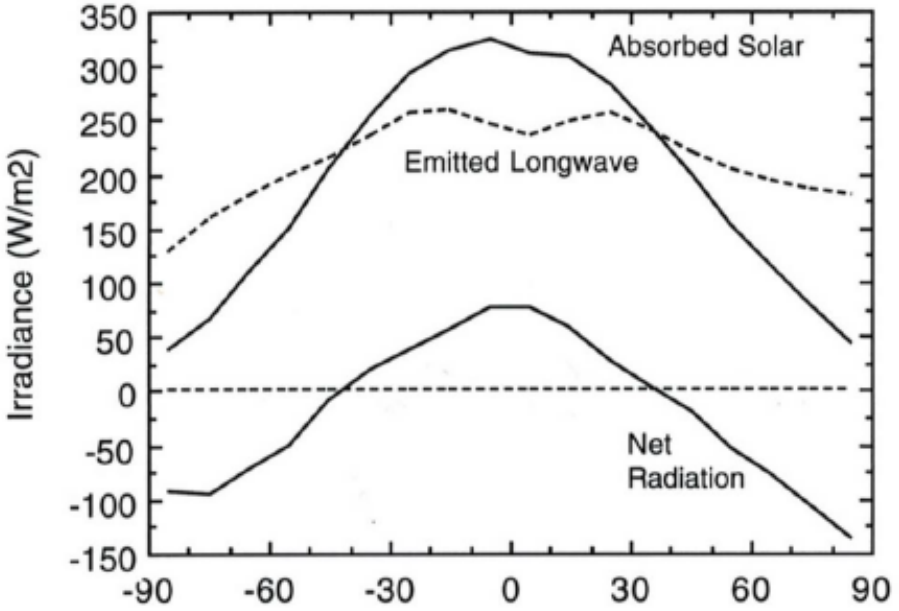

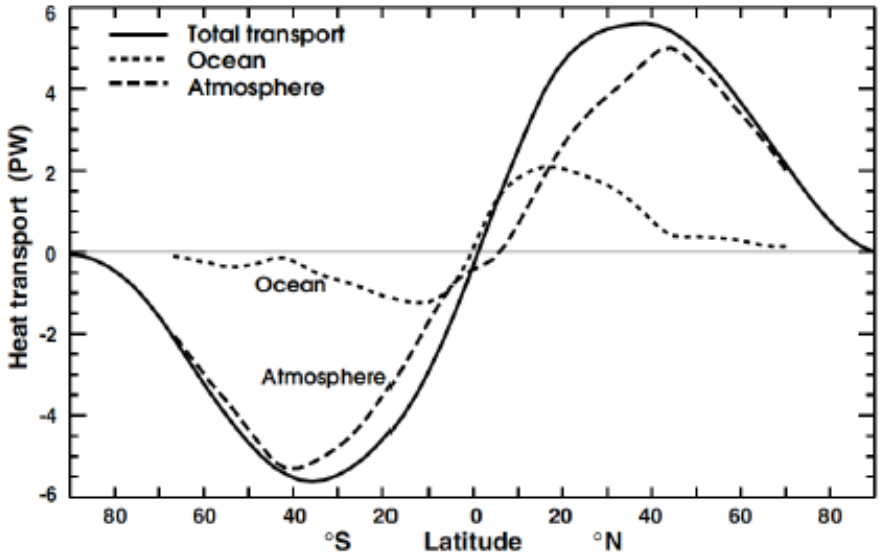

$$Q_{\mathrm{ABS}}(x,T_s) - F_{\infty}^{\uparrow}(x,T_s) = \Delta F_{\mathrm{ao}}(x,T_s)$$

Ice-Albedo feedback – Budyko model

$$Q_{\mathrm{ABS}}(x,T_s) - F_{\infty}^{\uparrow}(x,T_s) = \Delta F_{\mathrm{ao}}(x,T_s)$$

$$Q_{\mathrm{ABS}}(x,T_s) = \frac{S_0}{4}\, s(x)\, a_p(x,T_s) \qquad \alpha_p = \begin{cases} \alpha_{\text{ice-free}}, & T_s > -10^{\circ}\mathrm{C} \\ \alpha_{\text{ice}}, & T_s < -10^{\circ}\mathrm{C} \end{cases}$$

$$F_{\infty}^{\uparrow}(x,T_s) = A + B\,T_s$$

$$\Delta F_{\mathrm{ao}})_{\mathrm{Budyko}} = \gamma\left(T_s - \tilde{T}_s\right)$$

$$A + BT_s \;+\; \gamma\left(T_s - \tilde{T}_s\right) = \frac{S_0}{4}\, s(x)\, a_p(x,x_i)$$

Ice-Albedo feedback

$$A + BT_s + \gamma\left(T_s - \tilde{T}_s\right) = \frac{S_0}{4}\, s(x)\, a_p(x, x_i)$$

Possible solutions:

- Stable and unstable
- Very sensitive to solar constant and model parameters γ and α_p

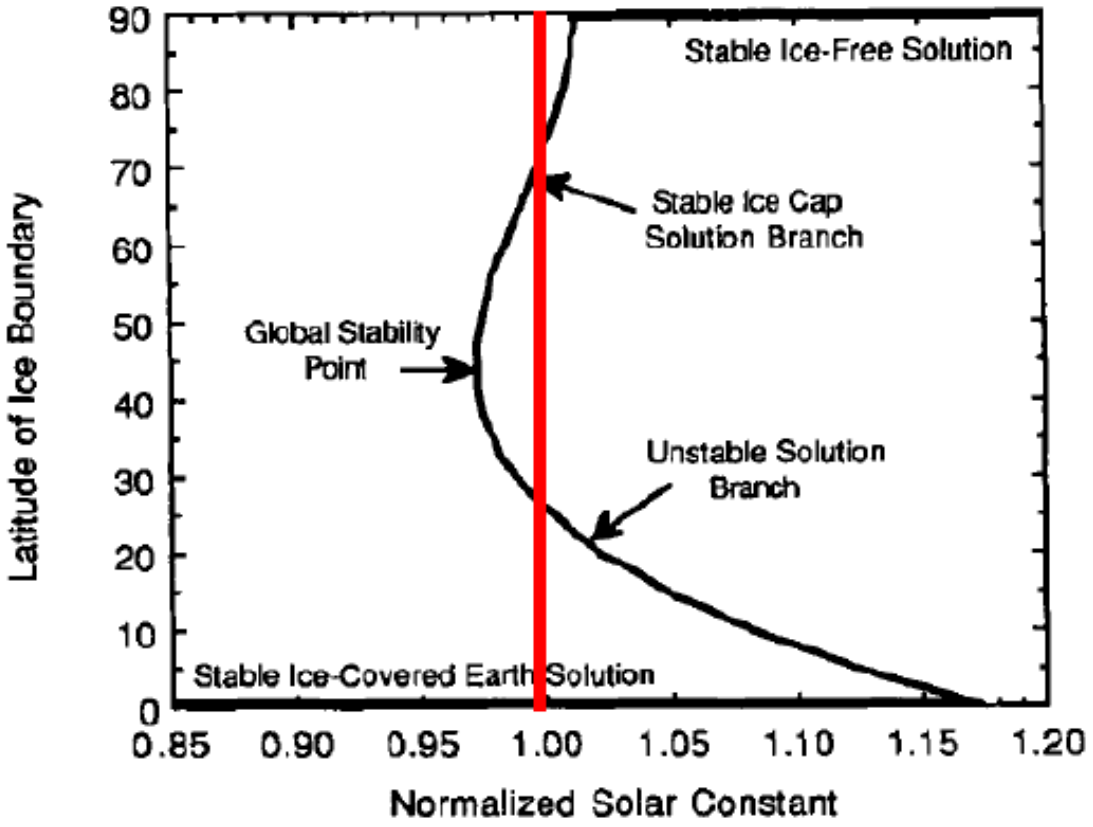

$$A + BT_s + \gamma\left(T_s - \tilde{T}_s\right) = \frac{S_0}{4}\, s(x)\, a_p(x, x_i)$$

$$I = \frac{(A + BT_s)}{(1/4)S_0} \qquad \delta = (\gamma/B).$$

$$I + \delta\left(I - \tilde{I}\right) = s(x)\, a_p(x, x_i)$$

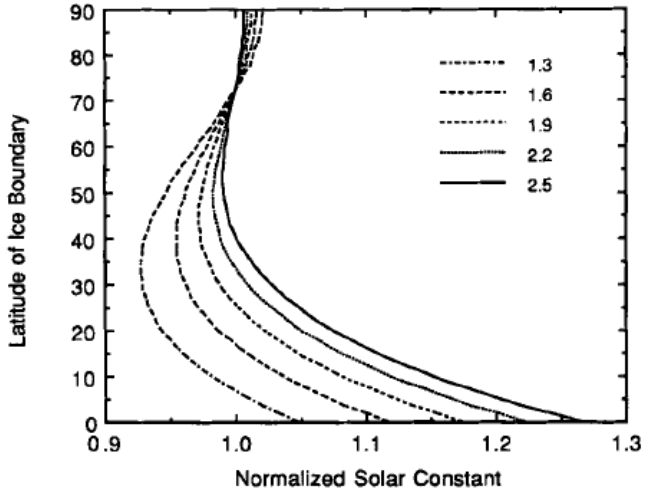

Fig. 9.6 Energy-balance climate model solution curves as in Fig. 9.5 for five values of the parameter δ, the ratio of the meridional transport coefficient to the longwave cooling coefficient. For larger δ the meridional temperature gradient is weaker and small changes in global-mean temperature are associated with larger displacements of the ice edge. Larger values of δ thus result in an ice cap whose area is more sensitive to solar constant.

$$\alpha_p = \begin{cases} \alpha_{\text{ice-free}}, & T_s > -10^\circ\text{C} \\ \alpha_{\text{ice}}, & T_s < -10^\circ\text{C} \end{cases}$$

$$a_p(x, x_i) = \begin{cases} a_0 + a_2 P_2(x), & T_s > -10^\circ\text{C}; \quad |x| < |x_i| \\ b_0, & T_s < -10^\circ\text{C}; \quad |x| > |x_i| \end{cases} \qquad (9.25)$$

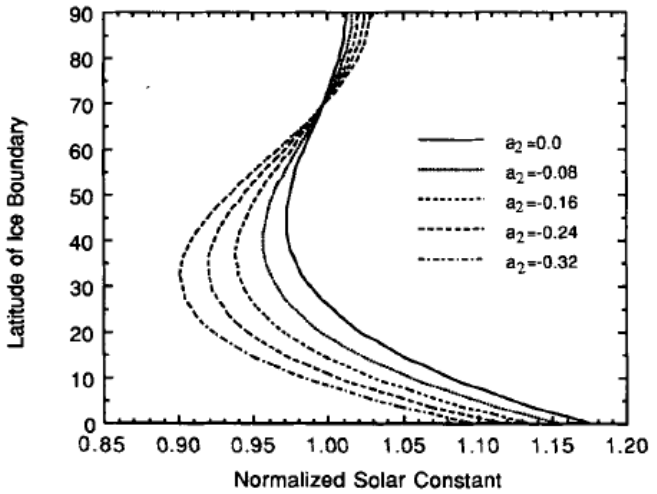

Fig. 9.7 Energy balance climate model solution curves as in Fig. 9.5 for five values of the parameter a_2, which measures the amount by which the ice-free planetary absorptivity decreases toward the poles. Larger negative values of a_2 weaken ice albedo feedback in high latitudes, since the albedo is then already fairly high even in the absence of icecover ($\delta = 1.9$).